

# Rotating Boson Stars and $Q$ -Balls

Burkhard Kleihaus, Jutta Kunz and Meike List\*

*Institut für Physik, Universität Oldenburg, Postfach 2503 D-26111 Oldenburg, Germany*

We consider axially symmetric, rotating boson stars. Their flat space limits represent spinning  $Q$ -balls. We discuss their properties and determine their domain of existence.  $Q$ -balls and boson stars are stationary solutions and exist only in a limited frequency range. The coupling to gravity gives rise to a spiral-like frequency dependence of the boson stars. We address the flat space limit and the limit of strong gravitational coupling. For comparison we also determine the properties of spherically symmetric  $Q$ -balls and boson stars.

PACS numbers: 04.40.-b, 11.17.+d

## I. INTRODUCTION

Non-topological solitons [1] or  $Q$ -balls [2] represent stationary localized solutions in flat space possessing a finite mass. In the simplest case they arise, when a complex scalar field has a suitable self-interaction, mimicking the interaction with other fields [1]. The global phase invariance of the scalar field theory is associated with a conserved charge  $Q$ , corresponding for instance to particle number [1].  $Q$ -balls thus represent non-topological solitons with charge  $Q$ .

Spherically symmetric  $Q$ -balls exist only in a certain frequency range,  $\omega_{\min} < \omega_s < \omega_{\max}$ , determined by the properties of the potential [1–3]. At a critical value of the frequency, both mass and charge of the  $Q$ -balls assume their minimal value, from where they monotonically rise towards both limiting values of the frequency. Considering the mass of the  $Q$ -balls as a function of the charge, there are thus two branches of  $Q$ -balls, merging and ending at the minimal charge and mass.  $Q$ -balls are stable along the lower branch, when their mass is smaller than the mass of  $Q$  free bosons [1].

When gravity is coupled to  $Q$ -balls, boson stars arise [3, 6–8]. The presence of gravity has crucial influence on the domain of existence of the classical solutions. Stationary spherically symmetric boson stars also exist only in a limited frequency range,  $\omega_0(\kappa) < \omega_s < \omega_{\max}$ , where  $\kappa$  denotes the strength of the gravitational coupling. They show, however, a different type of critical behaviour. For the smaller frequencies the boson stars exhibit a spiral-like frequency dependence of the charge and the mass, approaching finite limiting values at the centers of the spirals. When the maximal value of the frequency is approached, the charge and the mass of the boson stars tend to zero [3, 6].

We here determine the dependence of the stationary spherically symmetric boson stars on the strength of the gravitational coupling  $\kappa$  and, in particular, determine the domain of existence of the boson stars as a function of  $\kappa$ , including the limit  $\kappa \rightarrow \infty$  and the flat space limit.

Recently, the existence of rotating  $Q$ -balls was demonstrated [4]. These correspond to stationary localized solutions in flat space possessing a finite mass and a finite angular momentum. Interestingly, their angular momentum is quantized,  $J = nQ$  [4, 5]. Possessing even or odd parity, their energy density forms one or more tori.

Rotating boson stars exhibit angular momentum quantization as well,  $J = nQ$  [5]. Previously they have been obtained only for potentials without solitonic flat space solutions, and only for a restricted frequency range [5, 9–11]. Here we consider rotating boson stars which possess flat space counterparts. Our main objectives are to clarify, whether rotating boson stars exhibit an analogous frequency dependence as non-rotating boson stars, and to determine their domain of existence. For that purpose, we compute numerically sequences of rotating boson stars for constant values of the gravitational coupling strength, focussing on fundamental solutions with rotational quantum number  $n = 1$  and even parity.

In section II we recall the action, the general equations of motion and the global charges. In section III we present the stationary axially symmetric ansatz for the metric and the scalar field, we evaluate the global charges within this Ansatz, and present the boundary conditions for the metric and scalar field functions. We discuss stationary spherically symmetric  $Q$ -ball and boson star solutions in section IV, and present our results for rotating  $Q$ -ball and boson star solutions in section V. Section VI gives our conclusions. In the Appendices we address two auxiliary

---

\*Present address: ZARM, Universität Bremen, Am Fallturm, D-28359 Bremen, Germany

functions employed in the numerical integration (A), we present the systems of differential equations (B) and the components of the stress-energy tensor (C).

## II. ACTION, EQUATIONS AND GLOBAL CHARGES

### A. Action

We consider the action of a self-interacting complex scalar field  $\Phi$  coupled to Einstein gravity

$$S = \int \left[ \frac{R}{16\pi G} - \frac{1}{2} g^{\mu\nu} (\Phi^*_{,\mu} \Phi_{,\nu} + \Phi^*_{,\nu} \Phi_{,\mu}) - U(|\Phi|) \right] \sqrt{-g} d^4x , \quad (1)$$

where  $R$  is the curvature scalar,  $G$  is Newton's constant, the asterisk denotes complex conjugation,

$$\Phi_{,\mu} = \frac{\partial \Phi}{\partial x^\mu} , \quad (2)$$

and  $U$  denotes the potential

$$U(|\Phi|) = \lambda |\Phi|^2 (|\Phi|^4 - a|\Phi|^2 + b) = \lambda (\phi^6 - a\phi^4 + b\phi^2) , \quad (3)$$

with  $|\Phi| = \phi$ . The potential is chosen such that nontopological soliton solutions [1], also referred to as  $Q$ -balls [2], exist in the absence of gravity. As seen in Fig. 1, the self-interaction of the scalar field has an attractive component, and the potential has a minimum,  $U(0) = 0$ , at  $\Phi = 0$  and a second minimum at some finite value of  $|\Phi|$ . The boson mass is given by  $m_B = \sqrt{\lambda b}$ .

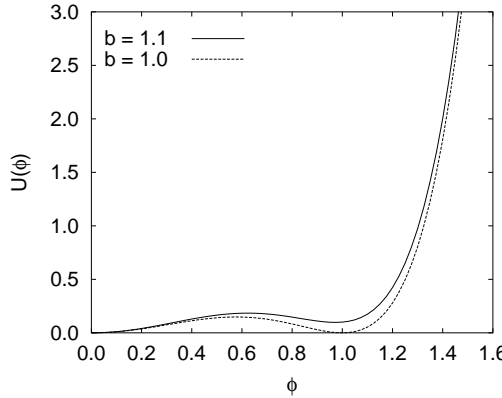


FIG. 1: The potential  $U(\phi)$  is shown for  $\lambda = 1$ ,  $a = 2$  and  $b = 1.1$  resp.  $b = 1$ .

### B. Equations

Variation of the action with respect to the metric leads to the Einstein equations

$$G_{\mu\nu} = R_{\mu\nu} - \frac{1}{2} g_{\mu\nu} R = \kappa T_{\mu\nu} , \quad (4)$$

with  $\kappa = 8\pi G$  and stress-energy tensor  $T_{\mu\nu}$

$$T_{\mu\nu} = g_{\mu\nu} L_M - 2 \frac{\partial L}{\partial g^{\mu\nu}} \quad (5)$$

$$= -g_{\mu\nu} \left[ \frac{1}{2} g^{\alpha\beta} (\Phi^*_{,\alpha} \Phi_{,\beta} + \Phi^*_{,\beta} \Phi_{,\alpha}) + U(\phi) \right] + (\Phi^*_{,\mu} \Phi_{,\nu} + \Phi^*_{,\nu} \Phi_{,\mu}) . \quad (6)$$

Variation with respect to the scalar field leads to the matter equation,

$$\left( \square + \frac{\partial U}{\partial |\Phi|^2} \right) \Phi = 0 , \quad (7)$$

where  $\square$  represents the covariant d'Alembert operator. Equations (4) and (7) represent the general set of Einstein–Klein–Gordon equations.

### C. Global Charges

The mass  $M$  and the angular momentum  $J$  of stationary asymptotically flat space-times can be obtained from their respective Komar expressions [12],

$$M = \frac{1}{4\pi G} \int_{\Sigma} R_{\mu\nu} n^{\mu} \xi^{\nu} dV , \quad (8)$$

and

$$\mathcal{J} = -\frac{1}{8\pi G} \int_{\Sigma} R_{\mu\nu} n^{\mu} \eta^{\nu} dV . \quad (9)$$

Here  $\Sigma$  denotes an asymptotically flat spacelike hypersurface,  $n^{\mu}$  is normal to  $\Sigma$  with  $n_{\mu} n^{\mu} = -1$ ,  $dV$  is the natural volume element on  $\Sigma$ ,  $\xi$  denotes an asymptotically timelike Killing vector field and  $\eta$  an asymptotically spacelike Killing vector field [12]. Replacing the Ricci tensor via the Einstein equations by the stress-energy tensor yields

$$M = 2 \int_{\Sigma} \left( T_{\mu\nu} - \frac{1}{2} g_{\mu\nu} T_{\gamma}^{\gamma} \right) n^{\mu} \xi^{\nu} dV , \quad (10)$$

and

$$\mathcal{J} = - \int_{\Sigma} \left( T_{\mu\nu} - \frac{1}{2} g_{\mu\nu} T_{\gamma}^{\gamma} \right) n^{\mu} \eta^{\nu} dV . \quad (11)$$

A conserved charge  $Q$  is associated with the complex scalar field  $\Phi$ , since the Lagrange density is invariant under the global phase transformation

$$\Phi \rightarrow \Phi e^{i\alpha} \quad (12)$$

leading to the conserved current

$$j^{\mu} = -i(\Phi^* \partial^{\mu} \Phi - \Phi \partial^{\mu} \Phi^*) , \quad j^{\mu}_{;\mu} = 0 . \quad (13)$$

## III. ANSATZ AND BOUNDARY CONDITIONS

### A. Ansatz

To obtain stationary axially symmetric solutions, we impose on the space-time the presence of two commuting Killing vector fields,  $\xi$  and  $\eta$ , where

$$\xi = \partial_t , \quad \eta = \partial_{\varphi} \quad (14)$$

in a system of adapted coordinates  $\{t, r, \theta, \varphi\}$ . In these coordinates the metric is independent of  $t$  and  $\varphi$ , and can be expressed in isotropic coordinates in the Lewis–Papapetrou form [13]

$$ds^2 = -f dt^2 + \frac{l}{f} \left[ g (dr^2 + r^2 d\theta^2) + r^2 \sin^2 \theta \left( d\varphi - \frac{\omega}{r} dt \right)^2 \right] . \quad (15)$$

The four metric functions  $f$ ,  $l$ ,  $g$  and  $\omega$  are functions of the variables  $r$  and  $\theta$  only.

The symmetry axis of the spacetime, where  $\eta = 0$ , corresponds to the  $z$ -axis. The elementary flatness condition [14]

$$\frac{X_{,\mu} X^{\mu}}{4X} = 1 , \quad X = \eta^{\mu} \eta_{\mu} \quad (16)$$

then imposes on the symmetry axis the condition [13]

$$g|_{\theta=0} = g|_{\theta=\pi} = 1 . \quad (17)$$

For the scalar field  $\Phi$  we adopt the stationary ansatz [5]

$$\Phi(t, r, \theta, \varphi) = \phi(r, \theta) e^{i\omega_s t + in\varphi} , \quad (18)$$

where  $\phi(r, \theta)$  is a real function, and  $\omega_s$  and  $n$  are real constants. Single-valuedness of the scalar field requires

$$\Phi(\varphi) = \Phi(2\pi + \varphi) , \quad (19)$$

thus the constant  $n$  must be an integer, i.e.,  $n = 0, \pm 1, \pm 2, \dots$ . We refer to  $n$  as rotational quantum number. When  $n \neq 0$ , the phase factor  $\exp(in\varphi)$  prevents spherical symmetry of the scalar field  $\Phi$ .

Thus to obtain stationary axially symmetric boson stars a system of five coupled partial differential equations needs to be solved. This set of equations is presented in Appendix B 2. In contrast, for the  $Q$ -balls of flat space the metric is the Minkowski metric, i.e.,  $f = l = g = 1$ ,  $\omega = 0$ . Here, at least in principle, only a single partial differential equation for the scalar field function needs to be solved.

For stationary spherically symmetric boson stars  $n = 0$ , and the scalar field function  $\phi$  depends only on the radial coordinate,  $\phi = \phi(r)$ . The metric then simplifies as well, since  $g \equiv 1$  and  $\omega \equiv 0$ , and the non-trivial metric functions  $f$  and  $l$  depend only on the radial coordinate,  $f = f(r)$ ,  $l = l(r)$ . Thus for stationary spherically symmetric solutions one obtains a much simpler system of three coupled ordinary differential equations. This set of equations is presented in Appendix B 1.

## B. Mass, angular momentum and charge

The mass  $M$  and the angular momentum  $J$  can be read off the asymptotic expansion of the metric functions  $f$  and  $\omega$ , respectively, [15]

$$f = 1 - \frac{2MG}{r} + O\left(\frac{1}{r^2}\right) , \quad \omega = \frac{2JG}{r^2} + O\left(\frac{1}{r^3}\right) , \quad (20)$$

i.e.,

$$M = \frac{1}{2G} \lim_{r \rightarrow \infty} r^2 \partial_r f , \quad J = \frac{1}{2G} \lim_{r \rightarrow \infty} r^2 \omega . \quad (21)$$

This is seen by considering the Komar expressions Eqs. (8) and (9), with unit vector  $n^{\mu} = (1, 0, 0, \omega/r)/\sqrt{f}$ , and volume element  $dV = 1/\sqrt{f}|g|^{1/2} dr d\theta d\varphi$ , leading to [16]

$$\begin{aligned} M &= -\frac{1}{8\pi G} \int_{\Sigma} R_t^t \sqrt{-g} dr d\theta d\varphi \\ &= \lim_{r \rightarrow \infty} \frac{2\pi}{8\pi G} \int_0^{\pi} \left[ \frac{\sqrt{l}}{f} r^2 \sin \theta \left( \frac{\partial f}{\partial r} - \frac{l}{f} \sin^2 \theta \omega \left( \frac{\partial \omega}{\partial r} - \frac{\omega}{r} \right) \right) \right]_r d\theta , \end{aligned} \quad (22)$$

and similarly

$$J = \lim_{r \rightarrow \infty} \frac{2\pi}{16\pi G} \int_0^{\pi} \left[ \frac{l^{3/2}}{f^2} r^2 \sin^3 \theta \left( \omega - r \frac{\partial \omega}{\partial r} \right) \right]_r d\theta . \quad (23)$$

Insertion of the asymptotic expansions of the metric functions then yields expressions (21).

Alternatively, the mass  $M$  and the angular momentum  $J$  can be obtained by direct integration of the expressions (10) and (11),

$$\begin{aligned} M &= \int_{\Sigma} (2T_{\mu}^{\nu} - \delta_{\mu}^{\nu} T_{\gamma}^{\gamma}) n_{\nu} \xi^{\mu} dV, \\ &= \int (2T_t^t - T_{\mu}^{\mu}) |g|^{1/2} dr d\theta d\varphi, \end{aligned} \quad (24)$$

corresponding to the Tolman mass, and

$$J = - \int T_{\varphi}^t |g|^{1/2} dr d\theta d\varphi. \quad (25)$$

The conserved scalar charge  $Q$  is obtained from the time-component of the current,

$$\begin{aligned} Q &= - \int j^t |g|^{1/2} dr d\theta d\varphi \\ &= 4\pi\omega_s \int_0^{\infty} \int_0^{\pi} |g|^{1/2} \frac{1}{f} \left(1 + \frac{n}{\omega_s} \frac{\omega}{r}\right) \phi^2 dr d\theta. \end{aligned} \quad (26)$$

From Eq. (25) for the angular momentum  $J$  and Eq. (26) for the scalar charge  $Q$ , one obtains the important quantization relation for the angular momentum,

$$J = nQ, \quad (27)$$

derived first by Schunck and Mielke [5], by taking into account that  $T_{\varphi}^t = nj^t$ , since  $\partial_{\varphi}\Phi = in\Phi$ . Thus a spherically symmetric boson star has angular momentum  $J = 0$ , because  $n = 0$ .

### C. Boundary conditions

The choice of appropriate boundary conditions must guarantee that the boson star solutions are globally regular and asymptotically flat, and that they possesses finite energy and finite energy density.

For spherically symmetric boson stars boundary conditions must be specified for the metric functions  $f(r)$  and  $l(r)$  and the scalar field function  $\phi(r)$  at the origin and at infinity. At the origin one finds the boundary conditions

$$\partial_r f|_{r=0} = 0, \quad \partial_r l|_{r=0} = 0, \quad \partial_r \phi|_{r=0} = 0. \quad (28)$$

Note, that for spherically symmetric boson stars the scalar field has a finite value  $\phi_0$  at the origin,

$$\phi(r) = \phi_0 + O(r^2). \quad (29)$$

For  $r \rightarrow \infty$  the metric approaches the Minkowski metric  $\eta_{\alpha\beta}$  and the scalar field assumes its vacuum value  $\Phi = 0$ . Accordingly, we impose at infinity the boundary conditions

$$f|_{r \rightarrow \infty} = 1, \quad l|_{r \rightarrow \infty} = 1, \quad \phi|_{r \rightarrow \infty} = 0. \quad (30)$$

For rotating axially symmetric boson stars appropriate boundary conditions must be specified for the metric functions  $f(r, \theta)$ ,  $l(r, \theta)$ ,  $g(r, \theta)$  and  $\omega(r, \theta)$ , and the scalar field function  $\phi(r, \theta)$  at the origin, at infinity, on the positive  $z$ -axis ( $\theta = 0$ ), and, exploiting the reflection symmetry w.r.t.  $\theta \rightarrow \pi - \theta$ , in the  $xy$ -plane ( $\theta = \pi/2$ ). At the origin we require

$$\partial_r f|_{r=0} = 0, \quad \partial_r l|_{r=0} = 0, \quad g|_{r=0} = 1, \quad \omega|_{r=0} = 0, \quad \phi|_{r=0} = 0. \quad (31)$$

At infinity the boundary conditions are

$$f|_{r \rightarrow \infty} = 1, \quad l|_{r \rightarrow \infty} = 1, \quad g|_{r \rightarrow \infty} = 1, \quad \omega|_{r \rightarrow \infty} = 0, \quad \phi|_{r \rightarrow \infty} = 0, \quad (32)$$

and for  $\theta = 0$  and  $\theta = \pi/2$ , respectively, we require the boundary conditions

$$\partial_{\theta} f|_{\theta=0} = 0, \quad \partial_{\theta} l|_{\theta=0} = 0, \quad g|_{\theta=0} = 1, \quad \partial_{\theta} \omega|_{\theta=0} = 0, \quad \phi|_{\theta=0} = 0, \quad (33)$$

and for even parity solutions

$$\partial_{\theta} f|_{\theta=\pi/2} = 0, \quad \partial_{\theta} l|_{\theta=\pi/2} = 0, \quad \partial_{\theta} g|_{\theta=\pi/2} = 0, \quad \partial_{\theta} \omega|_{\theta=\pi/2} = 0, \quad \partial_{\theta} \phi|_{\theta=\pi/2} = 0, \quad (34)$$

while for odd parity solutions  $\phi|_{\theta=\pi/2} = 0$ .

#### IV. STATIONARY SPHERICALLY SYMMETRIC SOLUTIONS

Stationary spherically symmetric solutions are obtained, when  $n = 0$ . The set of coupled non-linear ordinary differential equations, given in Appendix B 1, is solved numerically [17], subject to the above boundary conditions, Eqs. (28)-(30). Because of the power law fall-off of the metric functions, we compactify space by introducing the compactified radial coordinate

$$\bar{r} = \frac{r}{1+r} . \quad (35)$$

The numerical calculations employ a collocation method for boundary-value ordinary differential equations, using the damped Newton scheme for a sequence of meshes, until the required accuracy is reached [17].

##### A. Solutions in flat space: $Q$ -balls

Spherically symmetric  $Q$ -balls have been studied before (see e.g. [1, 2, 4], or [3] for a review). We here review their main features, to be able to better demonstrate the effects of gravity and rotation.

Recalling first the mass  $M$  of the  $Q$ -balls,

$$M = 4\pi \int_0^\infty T_{tt} r^2 dr = 4\pi \int_0^\infty [\omega_s^2 \phi^2 + \phi'^2 + U(\phi)] r^2 dr , \quad (36)$$

where the prime denotes differentiation with respect to  $r$ , and and their charge  $Q$ ,

$$Q(\omega_s) = 8\pi \omega_s \int_0^\infty \phi^2 r^2 dr , \quad (37)$$

we follow the discussion in [4] to obtain the limits for the frequency  $\omega_s$

$$\omega_{\min}^2 < \omega_s^2 < \omega_{\max}^2 , \quad (38)$$

while correcting for the missing factor of two in the field equation [18, 19]. The equation of motion for the scalar field [18],

$$0 = \phi'' + \frac{2}{r} \phi' - \frac{1}{2} \frac{dU(\phi)}{d\phi} + \omega_s^2 \phi , \quad (39)$$

is equivalent to [18]

$$\frac{1}{2} \phi'^2 + \frac{1}{2} \omega_s^2 \phi^2 - \frac{1}{2} U = \mathcal{E} - 2 \int_0^r \frac{\phi'^2}{r} dr , \quad (40)$$

where  $\mathcal{E}$  is an integration constant, and effectively describes a particle moving with friction in the potential [18]

$$V(\phi) = \frac{1}{2} \omega_s^2 \phi^2 - \frac{1}{2} U(\phi) . \quad (41)$$

The first necessary condition for  $Q$ -balls to exist is then  $V''(0) < 0$  [4] and yields the maximal frequency  $\omega_{\max}$  [18]

$$\omega_s^2 < \omega_{\max}^2 \equiv \frac{1}{2} U''(0) = \lambda b , \quad (42)$$

while the second condition is that  $V(\phi)$  should become positive for some non-zero value of  $\phi$  [4], i.e., [18]

$$\omega_s^2 > \omega_{\min}^2 \equiv \min_\phi [U(\phi)/\phi^2] = \lambda \left( b - \frac{a^2}{4} \right) . \quad (43)$$

Turning now to the  $Q$ -ball solutions, we specify the potential parameters as [4]

$$\lambda = 1 , \quad a = 2 , \quad b = 1.1 . \quad (44)$$

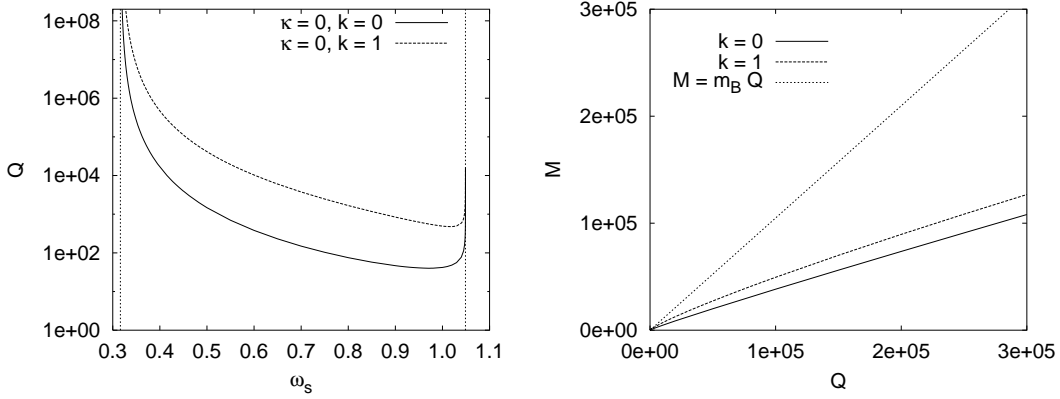


FIG. 2: Left: The charge  $Q$  is shown as a function of the frequency  $\omega_s$  for fundamental  $Q$ -balls ( $k = 0$ ) and their first radial excitations ( $k = 1$ ). Also shown are the limiting values of the frequency,  $\omega_{\min}$  and  $\omega_{\max}$ . Right: The mass  $M$  is shown as a function of the charge  $Q$  for fundamental  $Q$ -balls ( $k = 0$ ) and their first radial excitations ( $k = 1$ ). Also shown is the mass for  $Q$  free bosons,  $M = m_B Q$ . The upper branches of the mass  $M$  are not discernible (on this scale) from the mass of  $Q$  free bosons.

Fixing the value of  $\omega_s$  in the allowed range, one obtains a sequence of  $Q$ -ball solutions, consisting of the fundamental  $Q$ -ball and its radial excitations [4]. The boson function  $\phi$  of the fundamental  $Q$ -ball has no nodes, while it has  $k$  nodes for the  $k$ -th radial excitation.

Focussing on the fundamental  $Q$ -ball solutions and their first radial excitations, we exhibit in Fig. 2 the dependence of the charge  $Q$  on the frequency  $\omega_s$ . As seen in the figure, at a critical value  $\omega_{\text{cr}}$  the charge assumes its minimal value  $Q_{\text{cr}}$ . The charge diverges both when  $\omega_s \rightarrow \omega_{\min}$  and when  $\omega_s \rightarrow \omega_{\max}$  [1].

Fig. 2 also exhibits the mass  $M$  as a function of the charge  $Q$ . The region close to the critical value  $Q_{\text{cr}}$  is exhibited in Fig. 3 for the fundamental  $Q$ -balls and their first radial excitations. The lower branches correspond to values of the frequency  $\omega_s < \omega_{\text{cr}}$ , while the upper branches represent the values  $\omega_s > \omega_{\text{cr}}$ . When the mass is smaller than the mass of  $Q$  free bosons,  $M < m_B Q$ , the solutions are stable [1]. When  $\omega_s \rightarrow \omega_{\max}$ , the upper branches approach the mass  $M = m_B Q$  of  $Q$  free bosons from above [1].

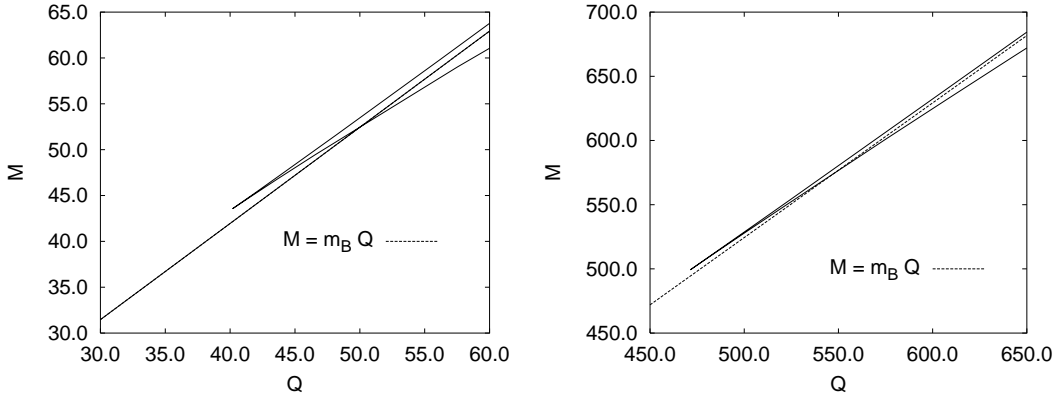


FIG. 3: The mass  $M$  is shown as a function of the charge  $Q$  for fundamental  $Q$ -balls ( $k = 0$ , left) and their first radial excitations ( $k = 1$ , right) in the region close to their corresponding critical values  $Q_{\text{cr}}$ . Also shown is the mass for  $Q$  free bosons,  $M = m_B Q$ .

The scalar field function  $\phi$  and the energy density  $T_{tt}$  of the fundamental  $Q$ -balls are shown in Fig. 4 for several values of the frequency  $\omega_s$  including  $\omega_{\text{cr}}$ . The energy density of the  $Q$ -balls is shell-like. Along the upper branch, with increasing charge and mass the maximum of the energy density decreases while moving outwards, whereas along the lower branch, with increasing charge and mass the maximum of the energy density increases while moving outwards, being strongly correlated with the steep fall-off of the scalar field function. Radially excited  $Q$ -balls with  $k$  nodes possess  $k + 1$  energy shells [4].

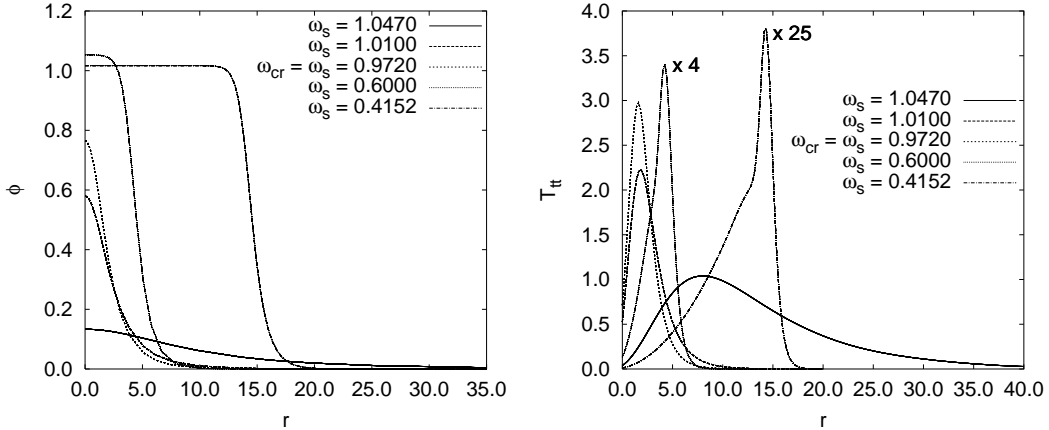


FIG. 4: The scalar field  $\phi(r)$  and the energy density  $T_{tt}(r)$  are shown for fundamental  $Q$ -balls ( $k = 0$ ) for several values of the frequency  $\omega_s$  including  $\omega_{\text{cr}}$ . For  $\omega_s = 0.6$  and  $\omega_s = 0.4152$  the scaled energy density  $T_{tt}(r)/4$  resp.  $T_{tt}(r)/25$  is shown.

### B. Solutions in curved space: boson stars

When the scalar field is coupled to gravity, boson stars arise (see e.g. [7, 9] for reviews). Spherically symmetric boson stars, based on a self-interacting boson field with a potential  $U$ , Eq. (3), have been considered by Friedberg, Lee, and Pang [6]. For their choice of the potential parameters the minima of the potential are degenerate, yielding for the minimum value of the frequency  $\omega_{\text{min}} = 0$ . In contrast, for our choice of parameters, Eq. (44), the potential has a global and a local minimum, and  $\omega_{\text{min}} > 0$ . The different form of the potential has consequences for some features of the boson stars, as discussed below.

To demonstrate the effects of gravity on the spherically symmetric solutions, we exhibit in Fig. 5 the charge  $Q$  as a function of the frequency  $\omega_s$  for the fundamental boson star solutions at a given value of the gravitational coupling constant  $\kappa$ .

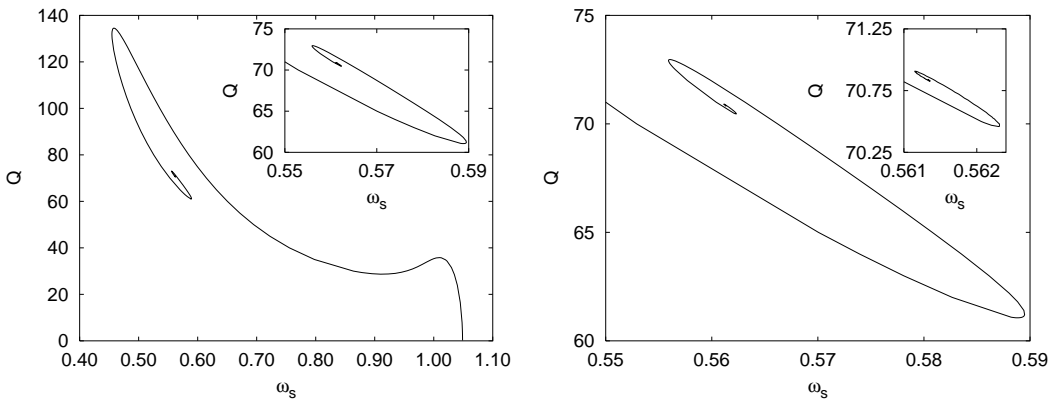


FIG. 5: The charge  $Q$  is shown as a function of the frequency  $\omega_s$  for fundamental boson stars ( $k = 0$ ) in the full range of existence (left), and in the frequency range of the spiral (right), for the gravitational coupling constant  $\kappa = 0.2$ .

For solutions in curved space the frequency  $\omega_s$  is also bounded from above by  $\omega_{\text{max}}$ , Eq. (42), since the scalar field exhibits asymptotically an exponential fall-off only for  $\omega_s < \omega_{\text{max}}$ . However, for the smaller values of  $\omega_s$  a new phenomenon occurs, as compared to flat space [6], where the solutions approach monotonically the limiting lower value  $\omega_{\text{min}}$ , Eq. (43). Denoting the minimal value of the frequency for boson stars by  $\omega_0(\kappa)$ , we observe that it differs from  $\omega_{\text{min}}$ , except for a single value of the gravitational coupling  $\kappa$ . For larger values of  $\kappa$ ,  $\omega_0(\kappa) > \omega_{\text{min}}$ , while for smaller values of  $\kappa$ ,  $\omega_0(\kappa) < \omega_{\text{min}}$ . (Note, that the latter case does not occur for a potential with degenerate minima, since there  $\omega_{\text{min}} = 0$ .) Moreover, in the presence of gravity the solutions do not approach monotonically the minimal value  $\omega_0(\kappa)$ . Instead one observes an inspiralling of the boson star solutions towards a limiting solution at the center of the spiral at a frequency  $\omega_{\text{lim}}(\kappa) > \omega_0(\kappa)$  [6].

In Fig. 6 we exhibit the charge  $Q$  as a function of the frequency  $\omega_s$ , for the fundamental boson star solution ( $k = 0$ )

for several values of the gravitational coupling constant  $\kappa$ , and also for the first radial excitation ( $k = 1$ ) for  $\kappa = 0.2$ . While the presence of a spiral is a genuine property of boson stars, the location and the size of the spiral depend on the gravitational coupling strength  $\kappa$  and on the node number  $k$ .

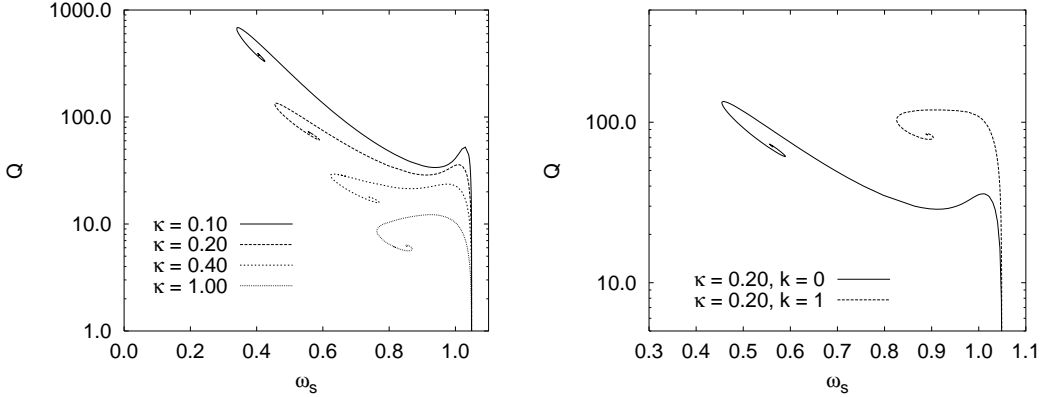


FIG. 6: The charge  $Q$  is shown as a function of the frequency  $\omega_s$  for fundamental boson stars ( $k = 0$ ) for the values of the gravitational coupling constant  $\kappa = 0.1, 0.2, 0.4, 1.0$  (left), and for their first radial excitations ( $k = 1$ ) for  $\kappa = 0.2$  (right).

The mass  $M$  has an analogous dependence on the frequency  $\omega_s$  as the charge  $Q$ , as seen in Fig. 7, where we also exhibit the frequency dependence of the value of the scalar field at the origin  $\phi(0)$ . The endpoints of  $\phi(0)$  in the figure correspond to the numerical values obtained closest to the centers of the spirals. We cannot decide numerically, however, whether the limiting solutions have indeed finite values  $\phi_{\lim}(0)$  [20].

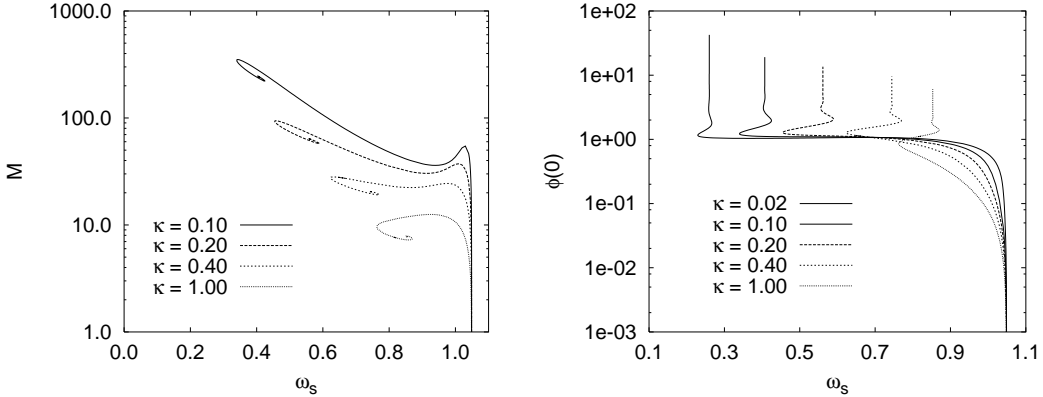


FIG. 7: The mass  $M$  (left) and the value of the scalar field at the origin  $\phi(0)$  (right) are shown as functions of the frequency  $\omega_s$  for fundamental boson stars ( $k = 0$ ) for the values of the gravitational coupling constant  $\kappa = 0.1, 0.2, 0.4, 1$  (left) resp.  $\kappa = 0.02, 0.1, 0.2, 0.4, 1$  (right).

When the mass  $M$  is considered as a function of the charge  $Q$ , we observe a cusp structure [6], as illustrated in Fig. 8. For smaller values of  $\kappa$  (e.g.,  $\kappa = 0.2$ ) we observe two sets of cusps. The first set of cusps is related to the single cusp present in flat space, which occurs at the minimal value of the charge  $Q_{\min}$ , where the upper and lower branch of the  $Q$ -ball merge. But whereas the upper branch extends infinitely far in flat space, it extends in curved space only up to a second cusp, reached at a second critical value of the charge, where this upper branch merges with a third branch extending down to zero. For larger values of  $\kappa$  (e.g.,  $\kappa = 1$ ) this set of two cusps, being a remainder of the flat space solutions, is no longer present.

The second set of cusps is related to the spirals, present only in curved space. Labelling these cusps of the spirals consecutively  $N = 1, 2, \dots$ , we exhibit the charge  $Q$ , the mass  $M$ , and the frequency  $\omega_s$  of the boson star solutions at these cusps in Table I, for several values of the gravitational coupling constant  $\kappa$ .

Focussing on the limiting solutions at the centers of the spirals, we exhibit in Table II the limiting values of the frequency  $\omega_{\lim}$ , the charge  $Q_{\lim}$  and the mass  $M_{\lim}$  for several values of the gravitational coupling constant  $\kappa$ . For

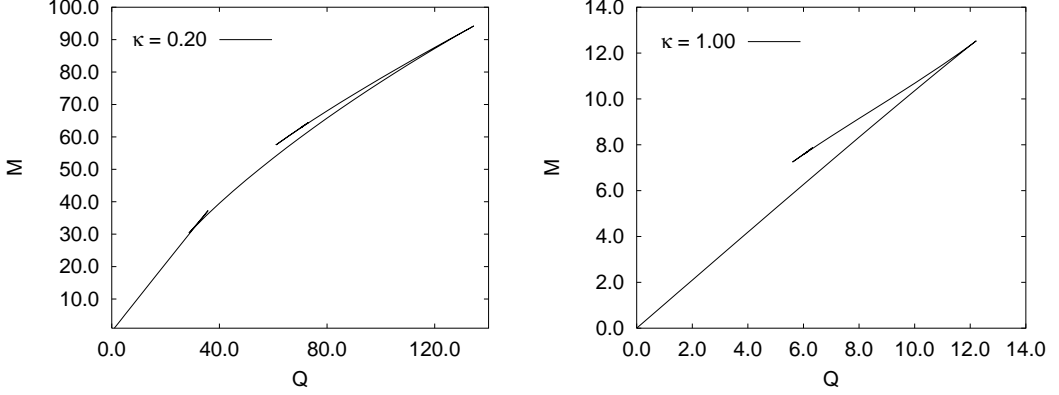


FIG. 8: The mass  $M$  is shown as a function of the charge  $Q$  for fundamental boson stars ( $k = 0$ ) for the values of the gravitational coupling constant  $\kappa = 0.2$  (left) and  $\kappa = 1$  (right).

$N$	$Q_N$	$M$	$\omega_s$	$N$	$Q_N$	$M$	$\omega_s$
1	685.5000	351.6320	0.34338	1	119.2400	122.9620	0.89402
2	331.3000	221.3990	0.42424	2	78.1580	88.3579	0.89343
3	391.9200	246.5870	0.40352	3	84.8980	94.4262	0.89000
4	378.2500	241.0480	0.40776	4	83.4960	93.1796	0.89067
5	380.8700	242.1160	0.40693	5	83.7470	93.4033	0.89047
6	380.4000	241.9250	0.40708	6	83.7090	93.3694	0.89048

$N$	$Q_N$	$M$	$\omega_s$	$N$	$Q_N$	$M$	$\omega_s$
1	29.3040	28.1273	0.63000	1	12.2180	12.5360	0.93000
2	15.7880	19.1084	0.76800	2	5.6059	7.24552	0.86000
3	17.8630	20.6836	0.74018	3	6.3314	7.87359	0.85305
4	17.4580	20.3833	0.74497	4	6.1911	7.75446	0.85290
5	17.5280	20.4361	0.74416	5	6.2148	7.77456	0.85304
6	17.5170	20.4273	0.74429	6	6.2108	7.77104	0.85302

TABLE I: Physical characteristics of the first six cusps of the fundamental boson star solutions ( $k = 0$ ) for gravitational coupling constants  $\kappa = 0.1$  (upper left),  $\kappa = 0.2$  (upper right),  $\kappa = 0.4$  (lower left),  $\kappa = 1$  (lower right).

small gravitational coupling we extract the following  $\kappa$ -dependence,

$$\begin{aligned}
 \omega_{\lim} &= c_0^\omega + c_1^\omega \kappa^{1/2} + c_2^\omega \kappa + O(\kappa^{3/2}), \\
 Q_{\lim} \kappa^{3/2} &= c_0^Q + c_1^Q \kappa^{1/2} + c_2^Q \kappa + O(\kappa^{3/2}), \\
 M_{\lim} \kappa^{3/2} &= c_0^M + c_1^M \kappa^{1/2} + c_2^M \kappa + O(\kappa^{3/2}),
 \end{aligned} \tag{45}$$

illustrated in Fig. 9. For small gravitational coupling we thus obtain a different  $\kappa$ -dependence, as compared to [6]. In particular, in the limit  $\kappa \rightarrow 0$  the limiting frequency  $\omega_{\lim}$  assumes a finite value,  $0 < \omega_{\lim}(0) < \omega_{\min}$ . We attribute this difference to the fact, that for a potential with degenerate minima, as employed in [6],  $\omega_{\min} = 0$ .

To address the  $\kappa$ -dependence of the domain of existence of the (fundamental) boson star solutions, corresponding to the interval  $[\omega_0(\kappa), \omega_{\max}]$ , we exhibit in Fig. 10 the charge  $Q$  as a function of the frequency  $\omega_s$  for a large set of values of the gravitational coupling constant  $\kappa$ , including the flat space limit. Interestingly, for values of the frequency  $\omega_s$  close to  $\omega_{\max}$ , the flat space values are not approached monotonically from below with decreasing  $\kappa$ . Here a weak coupling to gravity can lead to an increase of the mass of the boson star solutions.

As  $\kappa$  increases,  $\omega_0(\kappa)$  tends to a finite value  $\omega_0(\infty)$ , smaller than  $\omega_{\max}$ . Fixing  $\omega_s \in [\omega_0(\infty), \omega_{\max}]$  we observe that the scalar field scales like  $1/\sqrt{\kappa}$  for large values of  $\kappa$ . In order to obtain the solutions in the limit  $\kappa \rightarrow \infty$ , we therefore introduce the scaled scalar field  $\hat{\phi}(r) = \sqrt{\kappa}\phi(r)$ . Substituting  $\phi(r)$  in the field equation and taking the limit  $\kappa \rightarrow \infty$ , we find that all terms non-linear in  $\hat{\phi}(r)$  vanish. Similarly, in the Einstein equations all terms of higher than second order in  $\hat{\phi}(r)$  vanish and the dependence on  $\kappa$  cancels. Thus we end up with a set of differential equations identical to the original one, except that  $\kappa = 1$  and  $U(\hat{\phi}) = \lambda b \hat{\phi}^2$ . Solving this set of differential equations for fixed  $\lambda b$  and

$\kappa$	$\omega_{\text{lim}}$	$Q_{\text{lim}}$	$M_{\text{lim}}$
1.0000	0.85302	6.2114	7.7718
0.4000	0.74427	17.5180	20.4285
0.2000	0.56135	70.8330	63.2038
0.1000	0.40707	380.4600	241.9480
0.0200	0.25981	$1.136 \cdot 10^4$	4433.790
0.0100	0.23529	$4.011 \cdot 10^4$	$1.401 \cdot 10^4$
0.0020	0.20754	$5.954 \cdot 10^5$	$1.802 \cdot 10^5$
0.0010	0.20172	$1.797 \cdot 10^6$	$5.262 \cdot 10^5$
0.0002	0.19451	$2.181 \cdot 10^7$	$6.119 \cdot 10^6$
$0.2 \cdot 10^{-5}$	0.18924	$2.326 \cdot 10^{10}$	$6.316 \cdot 10^9$

TABLE II: Physical characteristics of the limiting solutions at the centers of the spirals for the fundamental boson stars ( $k = 0$ ) for a set of decreasing values of the gravitational coupling constant  $\kappa$ .

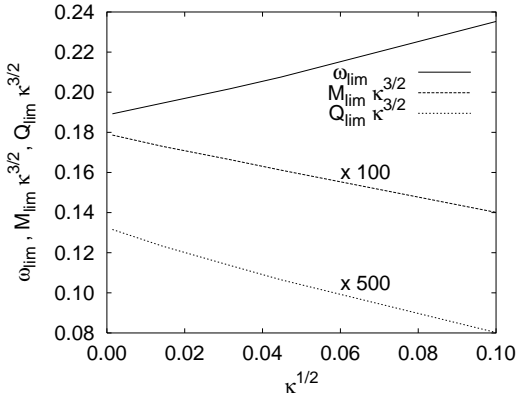


FIG. 9: The dependence of the frequency  $\omega_{\text{lim}}$ , the mass  $M_{\text{lim}}$  and the charge  $Q_{\text{lim}}$  of the limiting solutions at the centers of the spirals on the gravitational coupling constant  $\kappa$  for fundamental boson stars ( $k = 0$ ) for small values of  $\kappa$ .

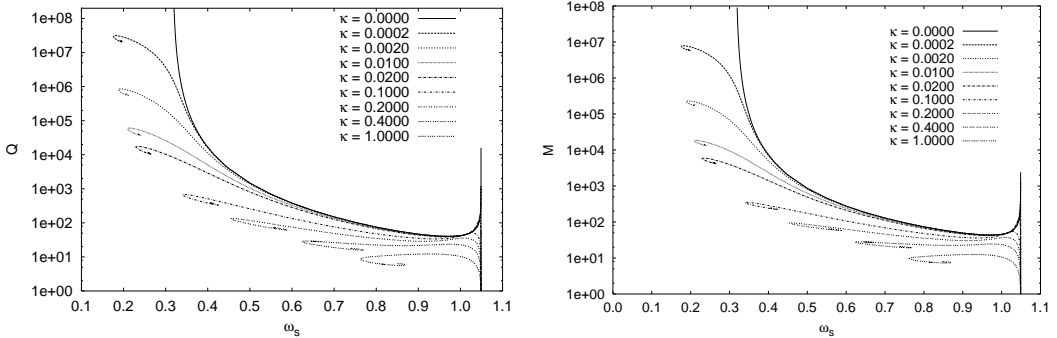


FIG. 10: The charge  $Q$  (left) and the mass  $M$  (right) are shown as functions of the frequency  $\omega_s$  for fundamental boson stars ( $k = 0$ ) for a set of decreasing values of the gravitational coupling constant  $\kappa$ . Also shown are the limiting flat space values.

varying  $\omega_s$ , we again find a spiral pattern for the (scaled) charge  $\hat{Q} = \kappa Q$ , shown in Fig. 11. This analysis yields

$$\omega_0(\infty) = 0.805, \quad \omega_{\text{lim}}(\infty) = 0.883.$$

Considering now the domain of existence in the limit  $\kappa \rightarrow 0$ , we note that we must distinguish two intervals here,  $[\omega_0(\kappa), \omega_{\text{min}}]$  and  $[\omega_{\text{min}}, \omega_{\text{max}}]$ . We observe from Fig. 10, that the limiting flat space values of the charge  $Q$  are approached in a continuously increasing interval, extending to the full interval  $[\omega_{\text{min}}, \omega_{\text{max}}]$  in the limit  $\kappa \rightarrow 0$ . In the interval  $[\omega_0(0), \omega_{\text{min}}]$  there are no flat space solutions, possessing finite charge or mass. As noted above, the limiting

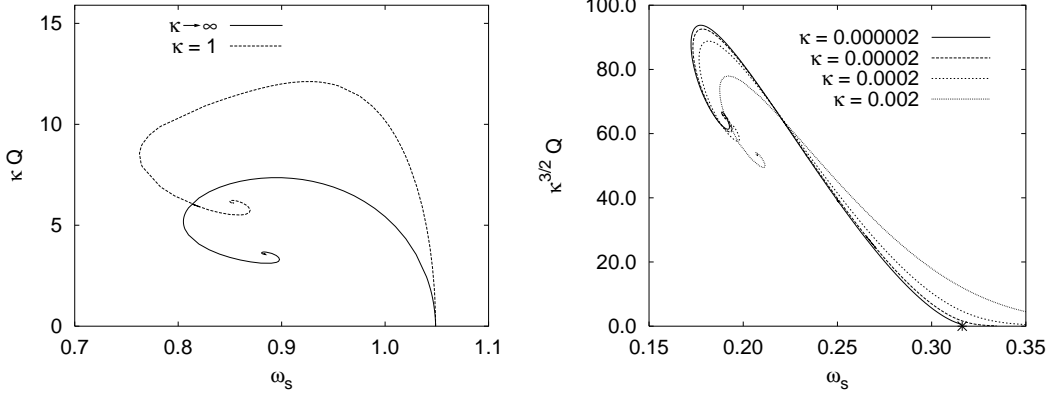


FIG. 11: Left: The scaled charge  $\kappa Q$  is shown as a function of the frequency  $\omega_s$  for fundamental boson stars ( $k = 0$ ) in the limit  $\kappa \rightarrow \infty$ . For comparison the scaled charge  $\kappa Q$  is also shown for  $\kappa = 1$ , resp.  $\kappa \rightarrow 0$  (right). Right: The scaled charge  $\kappa^{3/2}Q$  is shown as a function of the frequency  $\omega_s$  for fundamental boson stars ( $k = 0$ ) for  $\kappa = 0.002, 0.0002, 0.00002$ , and  $0.000002$ . The asterisk marks  $\omega_{\min}$ .

values of the charge  $Q_{\lim}$  and the mass  $M_{\lim}$  at the centers of the spirals diverge with  $\kappa^{-3/2}$ , when  $\kappa \rightarrow 0$ . We therefore determine the properties of the solutions in the limit  $\kappa \rightarrow 0$  in the interval  $[\omega_0(0), \omega_{\min}]$  by scaling the charge and the mass with  $\kappa^{3/2}$  for a sequence of solutions, corresponding to decreasing values of  $\kappa$ . Convergence towards the limiting values of the scaled charge is demonstrated in Fig. 11 [21]. Thus also in the limit  $\kappa \rightarrow 0$  we find a spiral pattern for the (scaled) charge  $\hat{Q} = \kappa^{3/2}Q$ . This analysis yields

$$\omega_0(0) = 0.172, \quad \omega_{\lim}(0) = 0.189.$$

We remark that for a potential with degenerate minima, as employed in [6], only the single interval  $[\omega_{\min}, \omega_{\max}]$  needs to be considered, since  $\omega_{\min} = 0$ , implying apparently  $\omega_0(0) = \omega_{\lim}(0) = \omega_{\min} = 0$ .

## V. ROTATING AXIALLY SYMMETRIC SOLUTIONS

Rotating axially symmetric solutions are obtained, when  $n \neq 0$ . We solve the set of coupled non-linear elliptic partial differential equations, given in Appendix B 2, numerically [22], subject to the above boundary conditions, Eqs. (31)-(34), employing the compactified radial coordinate, Eq. (35). The numerical calculations are based on the Newton-Raphson method. The equations are discretized on a non-equidistant grid in  $\bar{r}$  and  $\theta$ . Typical grids used have sizes  $100 \times 20$ , covering the integration region  $0 \leq \bar{r} \leq 1$  and  $0 \leq \theta \leq \pi/2$ .

### A. Rotating $Q$ -balls

The existence of rotating  $Q$ -balls has been shown by Volkov and Wöhner [4]. Based on the ansatz (18) for the scalar field  $\Phi$  [5], one obtains for rotating  $Q$ -ball solutions the field equation [18]

$$\left( \frac{\partial^2}{\partial r^2} + \frac{2}{r} \frac{\partial}{\partial r} + \frac{1}{r^2} \frac{\partial^2}{\partial \theta^2} + \frac{\cos \theta}{r^2 \sin \theta} \frac{\partial}{\partial \theta} - \frac{n^2}{r^2 \sin^2 \theta} + \omega_s^2 \right) \phi = \frac{1}{2} \frac{dU(\phi)}{d\phi}, \quad (46)$$

the mass [4]

$$M = 2\pi \int_0^\infty \int_0^\pi \left( \omega_s^2 \phi^2 + (\partial_r \phi)^2 + \frac{1}{r^2} (\partial_\theta \phi)^2 + \frac{n^2 \phi^2}{r^2 \sin^2 \theta} + U(\phi) \right) r^2 dr \sin \theta d\theta, \quad (47)$$

and the charge

$$Q = 4\pi \omega_s \int_0^\infty \int_0^\pi \phi^2 r^2 dr \sin \theta d\theta. \quad (48)$$

Their angular momentum satisfies the quantization relation  $J = nQ$ .

In their pioneering study [4] Volkov and Wöhnert show, that for a given value of  $n$  there are two types of solutions, possessing different parity. They exhibit examples of fundamental rotating  $Q$ -balls with quantum numbers  $n = 1 - 3$ , and both even and odd parity. They do not study the frequency dependence of rotating  $Q$ -ball solutions, however.

We illustrate the scalar field  $\phi(r, \theta)$  and the energy density  $T_{tt}(r, \theta)$  of fundamental rotating  $Q$ -balls with charge  $Q = 410$ , quantum numbers  $n = 1$  and  $2$ , and even parity in Figs. 12 and 13. For rotating  $Q$ -balls the scalar field  $\phi$  must vanish at the origin, as seen in Eq. (47). The energy density  $T_{tt}$  of even parity rotating  $Q$ -balls is torus-like. (For odd parity a double torus arises [4].) The mass  $M$ , the angular momentum  $J$  and the frequency  $\omega_s$  of these

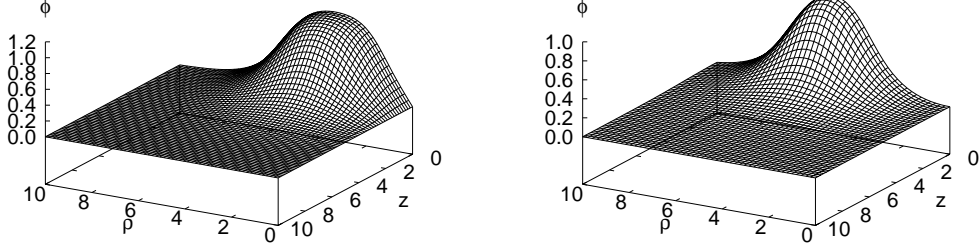


FIG. 12: The scalar field  $\phi(r, \theta)$  for fundamental rotating  $Q$ -balls with charge  $Q = 410$  and quantum number  $n = 1$  (left) and  $n = 2$  (right) is shown as a function of the coordinates  $\rho = r \sin \theta$  and  $z = r \cos \theta$ .

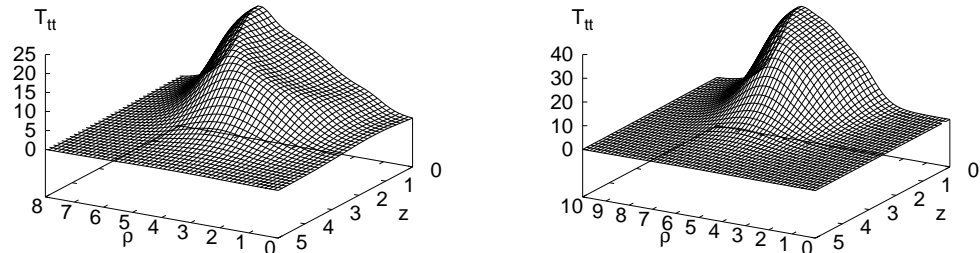


FIG. 13: The energy density  $T_{tt}$  for fundamental rotating  $Q$ -balls with charge  $Q = 410$  and quantum number  $n = 1$  (left) and  $n = 2$  (right) is shown as a function of the coordinates  $\rho = r \sin \theta$  and  $z = r \cos \theta$ .

rotating  $Q$ -balls are exhibited in Table III together with the properties of the corresponding non-rotating  $Q$ -ball. The properties of radially excited rotating  $Q$ -balls have not yet been studied [4].

$n$	$\omega_s$	$J$	$M$
0	0.5927	0	293.8
1	0.6931	410	363.4
2	0.7940	820	414.7

TABLE III: Physical properties of fundamental  $Q$ -balls with charge  $Q = 410$  and quantum numbers  $n = 0 - 2$ .

We here address the frequency dependence of rotating  $Q$ -ball solutions. We focus on fundamental rotating  $Q$ -balls with quantum number  $n = 1$  and even parity. In Fig. 14 we show the charge  $Q$  as a function of the frequency  $\omega_s$  for these fundamental rotating  $Q$ -balls. We observe the same upper limiting value  $\omega_{\max}$ , Eq. (42), for the frequency  $\omega_s$ , as for non-rotating  $Q$ -balls, which again ensures asymptotically an exponential fall-off of the scalar field  $\phi$ . For a given frequency  $\omega_s$  the charge of a rotating  $Q$ -ball is larger than the charge of a non-rotating  $Q$ -ball. We thus conjecture, that the frequency of rotating  $Q$ -balls is also limited by the minimal frequency  $\omega_{\min}$ , Eq. (43). Unfortunately, for

rotating  $Q$ -balls the numerical accuracy decreases considerably for large values of the charge  $Q$ , refraining us from approaching  $\omega_{\min}$  more closely.

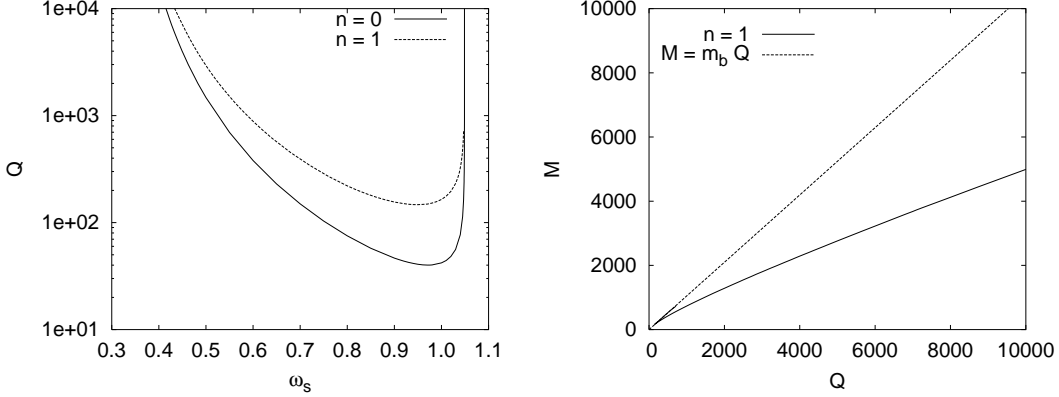


FIG. 14: The charge  $Q$  is shown as a function of the frequency  $\omega_s$  (left) and the mass  $M$  is shown as a function of the charge  $Q$  (right) for fundamental rotating  $Q$ -balls with quantum number  $n = 1$ . For comparison, the charge  $Q$  and the mass  $M$  also shown for fundamental non-rotating  $Q$ -balls. The upper branches of the mass  $M$  are not discernible (on this scale) from the mass of  $Q$  free bosons,  $M = m_b Q$  (right).

The mass of the rotating  $Q$ -balls shows the same cusp structure as the mass of non-rotating  $Q$ -balls. Only the minimal charge  $Q_{\min}$  of the rotating  $Q$ -balls is larger than the minimal charge of the non-rotating  $Q$ -balls,  $Q_{\min}(n = 1) > Q_{\min}(n = 0)$ . We conclude, that the set of rotating  $Q$ -balls exhibits the same general pattern as the set of non-rotating  $Q$ -balls.

### B. Rotating boson stars

We now turn to rotating boson stars, obtained when gravity is coupled to the rotating  $Q$ -ball solutions. We expect that the set of rotating boson stars also exhibits the same general pattern as the set of non-rotating boson stars. Previously [5, 11] rotating boson stars were obtained (only for a  $\Phi^4$ -potential and) only for a limited range of the frequency  $\omega_s$ . Therefore neither a spiral structure nor cusps were observed.

We here focus on fundamental rotating boson stars with rotational quantum number  $n = 1$  and even parity. We exhibit in Fig. 15 the charge  $Q$  as a function of the frequency  $\omega_s$  for fundamental rotating and non-rotating boson stars at gravitational coupling  $\kappa = 0.2$ .

Again, the frequency  $\omega_s$  of the solutions is bounded from above by  $\omega_{\max}$ , Eq. (42), ensuring an asymptotically exponential fall-off of the scalar field. Furthermore, as for the non-rotating boson stars, we observe for the rotating boson stars for the smaller values of the frequency  $\omega_s$  a backbending toward larger values of  $\omega_s$ , leading apparently also to an inspiralling of the solutions towards a limiting solution. Unfortunately, numerical accuracy does not allow a better determination of the spiral and the corresponding limiting values. Comparison of the rotating and non-rotating sets of solutions shows that the location of the spiral of the rotating solutions is shifted towards larger values of the frequency  $\omega_s$ .

The mass  $M$  has an analogous dependence on the frequency  $\omega_s$  as the charge  $Q$ , as seen in Fig. 15. When the mass  $M$  of the rotating boson stars is considered as a function of the charge  $Q$ , we observe an analogous cusp structure as for the non-rotating boson stars, as illustrated in Fig. 16. For smaller values of  $\kappa$  (e.g.,  $\kappa = 0.2$ ) we observe two sets of cusps. The first set of cusps is again related to the cusp present in flat space, occurring at the minimal value of the charge  $Q_{\min}$ , where the upper and lower branch of the rotating  $Q$ -ball merge. In curved space the upper branch extends again only up to a second cusp, reached at another critical value of the charge, where this upper branch merges with a third branch extending down to zero. For larger values of  $\kappa$  (e.g.,  $\kappa = 1$ ) this set of two cusps, being a remainder of the flat space solutions, is no longer present.

The second set of cusps is again related to the spirals, present only in curved space. Labelling these cusps again consecutively  $N = 1, 2, \dots$ , we exhibit the charge  $Q$ , the mass  $M$ , and the frequency  $\omega_s$  of the boson star solutions at the first two cusps in Table IV, for the gravitational coupling constants  $\kappa = 0.1, 0.2$ , and  $0.3$ . Numerical problems inhibit a better resolution of this cusp structure (with regard to the larger values of  $N$ ).

Addressing finally the  $\kappa$ -dependence of the domain of existence of the rotating boson star solutions, we exhibit in Fig. 17 the charge  $Q$  and the mass  $M$  as functions of the frequency  $\omega_s$  for several values of the gravitational coupling

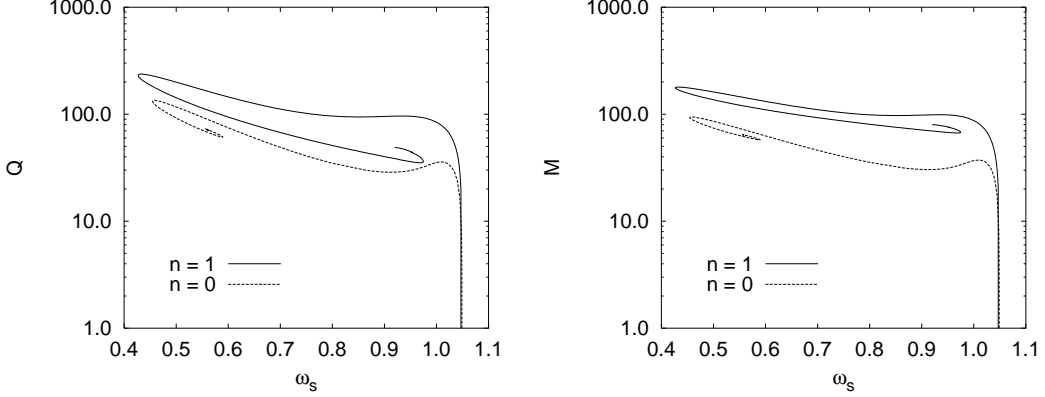


FIG. 15: The charge  $Q$  (left) and the mass  $M$  (right) are shown as functions of the frequency  $\omega_s$  for fundamental rotating ( $n = 1$ ) and non-rotating boson stars at the gravitational coupling  $\kappa = 0.2$ .

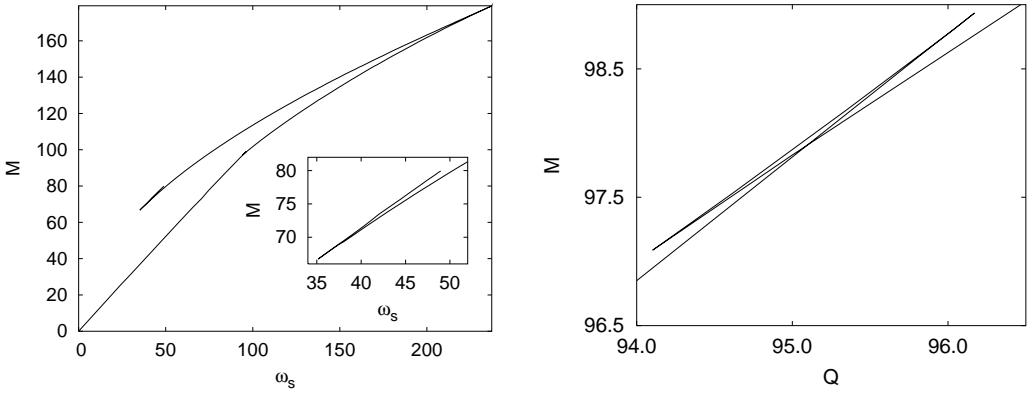


FIG. 16: The mass  $M$  is shown as a function of the charge  $Q$  for fundamental rotating ( $n = 1$ ) boson stars in the full range of existence (left), and in the charge range of the first set of cusps (right), for the gravitational coupling constant  $\kappa = 0.2$ .

$N$	$Q_N$	$M$	$J$	$\omega_s$
1	237.2	179.3	237.3	0.4325
2	35.2	66.7	35.1	0.9700
$N$	$Q_N$	$M$	$J$	$\omega_s$
1	111.0	99.3	111.0	0.5100
2	23.3	44.4	23.3	0.9700
$N$	$Q_N$	$M$	$J$	$\omega_s$
1	910.9	516.5	911.1	0.3400
2	76.4	138.8	75.7	0.9450

TABLE IV: Physical characteristics of the first two cusps of the fundamental rotating ( $n = 1$ ) boson star solutions for gravitational coupling constants  $\kappa = 0.1$  (upper),  $\kappa = 0.2$  (second), and  $\kappa = 0.3$  (third). Deviations from the relation  $J = nQ$  are due to numerical inaccuracy.

constant  $\kappa$ , including the flat space limit. Again, we observe that for values of the frequency  $\omega_s$  close to  $\omega_{\max}$ , the flat space values are not approached monotonically from below with decreasing  $\kappa$ .

We observe from Fig. 17 that also rotating ( $n = 1$ ) boson stars exist only in an interval  $[\omega_0(\kappa), \omega_{\max}]$ . To obtain the lower bound  $\omega_0(\kappa)$  in the limit  $\kappa \rightarrow \infty$ , we again introduce the scaled scalar field  $\hat{\phi}(r) = \sqrt{\kappa}\phi(r)$ , and substitute  $\phi(r)$  in the field equations. Taking the limit  $\kappa \rightarrow \infty$ , and solving the new set of differential equations, we find for the rotating ( $n = 1$ ) boson stars the lower bound  $\omega_0(\infty) = 0.677$ . The (scaled) charge  $\hat{Q} = \kappa Q$  of these solutions is shown

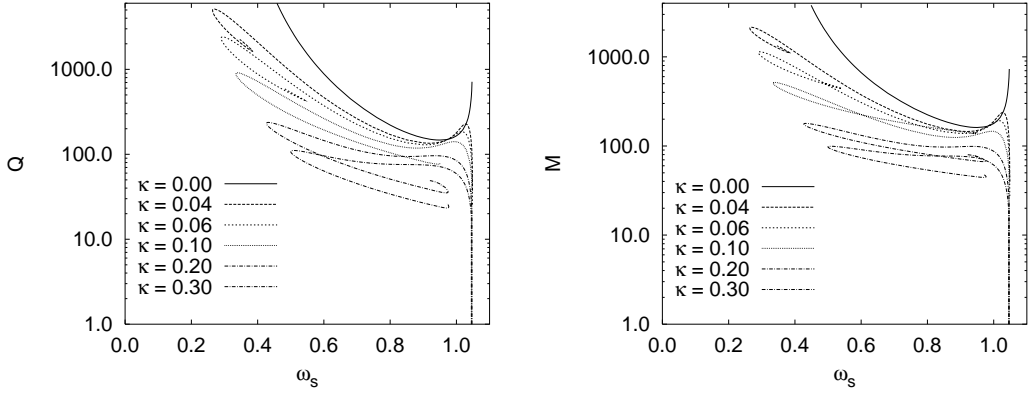


FIG. 17: The charge  $Q$  (left) and the mass  $M$  (right) are shown as functions of the frequency  $\omega_s$  for the fundamental rotating ( $n = 1$ ) boson stars for several values of the gravitational coupling constant  $\kappa$ . Also shown are the limiting flat space values.

in Fig. 18. Concerning the domain of existence in the limit  $\kappa \rightarrow 0$ , we expect a similar pattern as for the non-rotating boson stars. For  $\kappa < 0.06$ , for instance, we observe that  $\omega_0(\kappa) < \omega_{\min}$ . Numerical problems, however, prevent us from obtaining reliable results for very small values of  $\kappa$ .

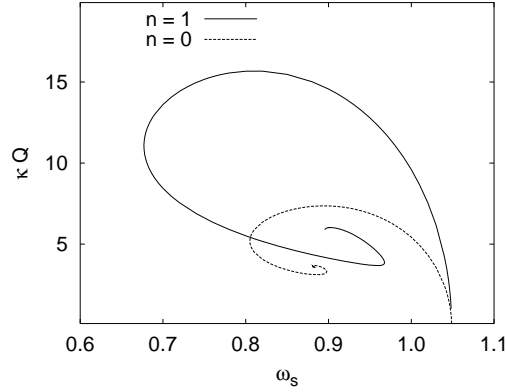


FIG. 18: The scaled charge  $\kappa Q$  is shown as a function of the frequency  $\omega_s$  for rotating ( $n = 1$ ) boson stars in the limit  $\kappa \rightarrow \infty$ . For comparison the scaled charge  $Q$  is also shown for non-rotating boson stars.

## VI. CONCLUSIONS

We have addressed boson stars and their flat space limit,  $Q$ -balls. To illustrate the effects of gravity and rotation, we have first recalled the main features of non-rotating  $Q$ -balls. Second, we have added gravity to obtain non-rotating boson stars. Third, we have added rotation to obtain rotating  $Q$ -balls, and finally we have added both gravity and rotation to obtain rotating boson stars. Our main emphasis has been to study the general pattern displayed by these regular extended objects, and to determine their domain of existence.

Spherically symmetric  $Q$ -balls and boson stars exist only in a limited frequency range. Whereas both mass and charge of  $Q$ -balls assume a minimal value at a critical frequency, from where they rise monotonically towards both smaller and larger frequencies, boson stars show a different type of behaviour. Their mass and charge tend to zero when the maximal frequency is approached, while for smaller values of the frequency charge and mass exhibit a spiral-like frequency dependence, leading to limiting solutions with finite values of the mass  $M_{\lim}$ , the charge  $Q_{\lim}$  and the frequency  $\omega_{\lim}$ , depending on the gravitational coupling constant  $\kappa$ .

Denoting the domain of existence of spherically symmetric boson stars by  $[\omega_0(\kappa), \omega_{\max}]$ , we observe, that when  $\kappa \rightarrow \infty$ , the lower limiting value of the frequency  $\omega_0(\kappa)$  tends to a finite value  $\omega_0(\infty) < \omega_{\max}$ , obtained by solving the set of field equations for the scaled scalar field  $\sqrt{\kappa}\phi(r)$ .

For small values of  $\kappa$ , on the other hand, the domain of existence consists of two parts,  $[\omega_0(\kappa), \omega_{\min}]$  and  $[\omega_{\min}, \omega_{\max}]$ .

In the limit  $\kappa \rightarrow 0$ , the lower limiting value of the frequency  $\omega_0(\kappa)$  tends to a finite value,  $\omega_0(0) < \omega_{\min}$ . In the interval  $[\omega_0(0), \omega_{\min}]$  there are no flat space solutions, possessing finite charge or mass. The limiting values of the spirals,  $Q_{\lim}$  and  $M_{\lim}$  diverge with  $\kappa^{-3/2}$  when  $\kappa \rightarrow 0$ . (For a potential with degenerate minima [6] only the single interval  $[\omega_{\min}, \omega_{\max}]$  needs to be considered, since  $\omega_{\min} = 0$ .)

Spherically symmetric  $Q$ -balls and boson stars possess radial excitations. Their systematic study has not yet been performed. We have, however, considered the first radial excitations of  $Q$ -balls and the first radial excitations of boson stars at a given gravitational coupling. This indicates, that radially excited  $Q$ -balls and boson stars possess an analogous frequency dependence and critical behaviour as the corresponding fundamental solutions.

Rotating  $Q$ -balls and boson stars possess a quantized angular momentum,  $J = nQ$ . For each rotational quantum number  $n$  there are even and odd parity solutions. Here we have focussed on solutions with  $n = 1$  and even parity. These rotating  $Q$ -balls show a frequency dependence and critical behaviour analogous to the non-rotating  $Q$ -balls. Likewise, the rotating boson stars show a frequency dependence and critical behaviour analogous to the non-rotating boson stars. In particular, on the one hand we observe that the mass and charge of rotating boson stars tend to zero when the maximal frequency is approached, and on the other hand we see a spiral-like frequency dependence for the mass and charge for the smaller values of the frequency. Unfortunately, numerical inaccuracies increase along the spirals, preventing a reliable construction of their interior parts.

Rotating ( $n = 1$ ) boson stars also exist only in an interval  $[\omega_0(\kappa), \omega_{\max}]$ . In the range of  $\kappa$  considered, the lower limiting value  $\omega_0(\kappa)$  of rotating boson star solutions is larger than the lower limiting value  $\omega_0(\kappa)$  of non-rotating boson star solutions. In the limit  $\kappa \rightarrow \infty$ , the lower bound  $\omega_0(\kappa)$  is again obtained by solving the set of field equations for the scaled scalar field  $\sqrt{\kappa}\phi(r)$ .

For small values of  $\kappa$ , we also observe an analogous pattern for the rotating boson stars as for the non-rotating boson stars. Numerical problems prevent us, however, from obtaining reliable results for the domain of existence for very small values of  $\kappa$ .

A systematic study of the frequency dependence of rotating boson stars with higher rotational quantum number  $n$  and with both parities is still missing and represents a numerical challenge. While the energy density of rotating boson stars with  $n = 1$  and even parity has a torus-like structure, the energy density of rotating boson stars with  $n = 1$  and odd parity should have a double-torus structure. For radially excited rotating boson stars the structure of the energy density may involve concentric tori. Their construction remains an open challenge, as well.

### Acknowledgments

B.K. gratefully acknowledges support by the DFG under contract KU612/9-1.

### APPENDIX A: AUXILIARY FUNCTIONS

In order to be able to calculate boson star solutions for a given value of the charge  $Q$ , we define 2 auxiliary functions,  $\rho(r, \theta)$  and  $\omega_s(r, \theta)$ . The equation of motion for the function  $\rho(r, \theta)$  consists of the Laplacian acting on  $\rho(r, \theta)$  and a source term, which is proportional to the charge density, Eq. (26),

$$\left( |g|^{1/2} g^{rr} \rho_{,r} \right)_{,r} + \left( |g|^{1/2} g^{\theta\theta} \rho_{,\theta} \right)_{,\theta} = -|g|^{1/2} \left( g^{tt} + g^{t\varphi} \frac{n}{\omega_s} \right) \phi^2. \quad (\text{A1})$$

Integration yields

$$\begin{aligned} \int_0^\pi \left( |g|^{1/2} g^{rr} \rho_{,r} \right) \Big|_0^\infty d\theta + \int_0^\infty \left( |g|^{1/2} g^{\theta\theta} \rho_{,\theta} \right) \Big|_0^\pi dr \\ = - \int_0^\infty \int_0^\pi |g|^{1/2} \left( g^{tt} + g^{t\varphi} \frac{n}{\omega_s} \right) \phi^2 dr d\theta, \quad (\text{A2}) \end{aligned}$$

and with  $|g|^{1/2} = l^{3/2} gr^2 \sin\theta/f$  and Eq. (26) we obtain

$$\int_0^\pi \left( \sin\theta l^{1/2} r^2 \rho_{,r} \right) \Big|_0^\infty d\theta + \int_0^\infty \left( \sin\theta l^{1/2} \rho_{,\theta} \right) \Big|_0^\pi dr = \frac{Q}{4\pi\omega_s}. \quad (\text{A3})$$

Making use of the asymptotic expansion for the function  $\rho(r, \theta)$ ,

$$\rho = \rho_\infty + \frac{C}{r} + O\left(\frac{1}{r^2}\right) + \dots, \quad (\text{A4})$$

with constants  $C$  and  $\rho_\infty$ , and thus asymptotically  $r^2 \rho_{,r} \rightarrow -C$ , we obtain

$$C \int_0^\pi \sin \theta d\theta = 2C = \frac{Q}{4\pi\omega_s}. \quad (\text{A5})$$

This then yields the connection between the function  $\rho(r, \theta)$  at infinity, the frequency  $\omega_s$  and the charge  $Q$ ,

$$\left( r^2 \rho_{,r} \omega_s - \frac{Q}{8\pi} \right) \Big|_{r \rightarrow \infty} = 0. \quad (\text{A6})$$

Since we cannot impose the value of the frequency  $\omega_s$ , when we impose the value of the charge, we need to solve for the frequency  $\omega_s$ . The frequency  $\omega_s$  is a constant. An adequate equation is therefore, that the Laplacian of  $\omega_s$  vanishes,

$$\left( |g|^{1/2} g^{rr} \omega_{s,r} \right)_{,r} + \left( |g|^{1/2} g^{\theta\theta} \omega_{s,\theta} \right)_{,\theta} = 0. \quad (\text{A7})$$

The appropriate set of boundary conditions for these two auxiliary functions are

$$\partial_r \omega_s|_{r=0} = 0, \quad 8\pi r^2 \rho_{,r} \omega_s|_{r \rightarrow \infty} = Q, \quad \partial_\theta \omega_s|_{\theta=0} = 0, \quad \partial_\theta \omega_s|_{\theta=\pi/2} = 0, \quad (\text{A8})$$

$$\partial_r \rho|_{r=0} = 0, \quad \rho|_{r \rightarrow \infty} = \rho_\infty, \quad \partial_\theta \rho|_{\theta=0} = 0, \quad \partial_\theta \rho|_{\theta=\pi/2} = 0, \quad (\text{A9})$$

and  $\rho_\infty$  is an arbitrary constant.

When instead of the charge  $Q$  a value for the frequency  $\omega_s$  is imposed, use of the auxiliary functions is not necessary, but convenient, since the charge is then obtained directly. In this case, the same set of boundary conditions is appropriate except for

$$\omega_s|_{r \rightarrow \infty} = \omega_\infty, \quad (\text{A10})$$

and  $\omega_\infty$  is the required value.

## APPENDIX B: SYSTEM OF DIFFERENTIAL EQUATIONS

### 1. Spherically symmetric solutions

For the spherically symmetric boson stars we obtain the following set of coupled non-linear ordinary differential equations

$$\begin{aligned} \partial_r^2 f &= -\frac{1}{2} \frac{1}{f l} \left[ 4\kappa f l^2 U(\phi) - 8\kappa \omega_s^2 l^2 \phi^2 + \frac{4}{r} f l \partial_r f - 2l \partial_r f \right. \\ &\quad \left. + f \partial_r l \partial_r f \right] \end{aligned} \quad (\text{B1})$$

$$\begin{aligned} \partial_r^2 l &= -\frac{1}{2} \frac{1}{f l} \left[ 8\kappa l^3 U(\phi) - 8\kappa \omega_s^2 \frac{l^3}{f} \phi^2 + \frac{6}{r} f l \partial_r l \right. \\ &\quad \left. - f (\partial_r l)^2 \right] \end{aligned} \quad (\text{B2})$$

$$\begin{aligned} \partial_r^2 \phi &= -\frac{1}{2} \frac{1}{f l} \left[ 2\omega_s^2 \frac{l^2}{f} \phi - l^2 \frac{\partial U(\phi)}{\partial \phi} + \frac{4}{r} f l \partial_r \phi \right. \\ &\quad \left. + f \partial_r l \partial_r \phi \right]. \end{aligned} \quad (\text{B3})$$

For the auxiliary functions the equations are

$$0 = -\frac{f}{l} \left( \partial_r^2 \rho + \frac{2}{r} \partial_r \rho + \frac{1}{2l} \partial_r l \partial_r \rho \right) + \frac{1}{f} \phi^2, \quad (\text{B4})$$

$$0 = \frac{f}{l} \left( \partial_r^2 \omega_s + \frac{2}{r} \partial_r \omega_s + \frac{1}{2l} \partial_r l \partial_r \omega_s \right). \quad (\text{B5})$$

## 2. Axially symmetric solutions

For the rotating boson stars we obtain the following set of coupled non-linear partial differential equations

$$\begin{aligned}
r^2 \partial_r^2 f + \partial_\theta^2 f &= -\frac{1}{2} \frac{1}{f l} \left[ 4\kappa r^2 f l^2 U(\phi) - 8\kappa n^2 l^2 g \omega^2 \phi^2 - 16\kappa r n \omega_s l^2 g \omega \phi^2 \right. \\
&\quad - 8\kappa r^2 \omega_s^2 l^2 g \phi^2 - 2 \sin^2 \theta l^2 \omega^2 + 4r f l \partial_r f \\
&\quad + 2 \frac{\cos \theta}{\sin \theta} f l \partial_\theta f + f l \partial_\theta f - 2l \left( r^2 (\partial_r f)^2 + (\partial_\theta f)^2 \right) \\
&\quad + r^2 f \partial_r l \partial_r f + 4r \sin^2 \theta l^2 \omega \partial_r \omega \\
&\quad \left. - 2 \sin^2 \theta l^2 \left( r^2 (\partial_r \omega)^2 + (\partial_\theta \omega)^2 \right) \right] \tag{B6}
\end{aligned}$$

$$\begin{aligned}
r^2 \partial_r^2 g + \partial_\theta^2 g &= -\frac{1}{2} \frac{1}{f l} \left[ -8\kappa n^2 f l g^2 \frac{1}{\sin^2 \theta} \phi^2 - 2 \sin^2 \theta \frac{l^2}{f} g \omega^2 \right. \\
&\quad + 8\kappa f l g (\partial_\theta \phi)^2 + 4r f l \partial_r g - 2 \frac{\cos \theta}{\sin \theta} f l \partial_\theta g \\
&\quad - 2 \frac{f l}{g} \left( r^2 (\partial_r g)^2 + (\partial_\theta g)^2 \right) + f \left( r^2 \partial_r l \partial_r g - \partial_\theta l \partial_\theta g \right) \\
&\quad + 2 \frac{l g}{f} (\partial_\theta f)^2 - 2 \frac{\cos \theta}{\sin \theta} f g \partial_\theta l - 3 \frac{f}{l} g (\partial_\theta l)^2 + 2 f g \partial_\theta^2 l \\
&\quad + 4r \sin^2 \theta \frac{l^2 g}{f} \omega \partial_r \omega \\
&\quad \left. - 2 \sin^2 \theta \frac{l^2 g}{f} \left( r^2 (\partial_r \omega)^2 + 2 (\partial_\theta \omega)^2 \right) \right] \tag{B7}
\end{aligned}$$

$$\begin{aligned}
r^2 \partial_r^2 l + \partial_\theta^2 l &= -\frac{1}{2} \frac{1}{f l} \left[ 8\kappa r^2 l^3 g U(\phi) + 8\kappa \frac{1}{\sin^2 \theta} n^2 f l^2 g \phi^2 - 8\kappa n^2 \frac{l^3 g}{f} \omega^2 \phi^2 \right. \\
&\quad - 16\kappa r n \omega_s \frac{l^3 g}{f} \omega \phi^2 - 8\kappa r^2 \omega_s^2 \frac{l^3 g}{f} \phi^2 + 6r f l \partial_r l \\
&\quad \left. + 4 \frac{\cos \theta}{\sin \theta} f l \partial_\theta l - f \left( r^2 (\partial_r l)^2 + (\partial_\theta l)^2 \right) \right] \tag{B8}
\end{aligned}$$

$$\begin{aligned}
r^2 \partial_r^2 \omega + \partial_\theta^2 \omega &= -\frac{1}{2} \frac{1}{f l} \left[ -8\kappa \frac{1}{\sin^2 \theta} n^2 f l g \omega \phi^2 - 8\kappa r \frac{1}{\sin^2 \theta} n \omega_s f l g \phi^2 \right. \\
&\quad - 4f l \omega + 4r f l \partial_r \omega + 6 \frac{\cos \theta}{\sin \theta} f l \partial_\theta \omega \\
&\quad - 4l \left( r^2 \partial_r f \partial_r \omega + \partial_\theta f \partial_\theta \omega \right) \\
&\quad + 3f \left( r^2 \partial_r l \partial_r \omega + \partial_\theta l \partial_\theta \omega \right) \\
&\quad \left. + 4r l \omega \partial_r f - 3r f \omega \partial_r l \right] \tag{B9}
\end{aligned}$$

$$\begin{aligned}
r^2 \partial_r^2 \phi + \partial_\theta^2 \phi = & -\frac{1}{2} \frac{1}{f l} \left[ -r^2 l^2 g \frac{\partial U(\phi)}{\partial \phi} - 2 \frac{1}{\sin^2 \theta} n^2 f l g \phi \right. \\
& + 2 \frac{l^2 g}{f} (\omega n + r \omega_s)^2 \phi + 4 r f l \partial_r \phi \\
& \left. + 2 \frac{\cos \theta}{\sin \theta} f l \partial_\theta \phi + f (r^2 \partial_r l \partial_r \phi + \partial_\theta l \partial_\theta \phi) \right]. \tag{B10}
\end{aligned}$$

For the auxiliary functions the equations are

$$\begin{aligned}
0 = & -\frac{f}{l g} \left( \partial_r^2 \rho + \frac{2}{r} \partial_r \rho + \frac{1}{2 l} \partial_r l \partial_r \rho \right) \\
& - \frac{1}{r^2} \frac{f}{l g} \left( \partial_\theta^2 \rho + \frac{\cos \theta}{\sin \theta} \partial_\theta \rho + \frac{1}{2 l} \partial_\theta l \partial_\theta \rho \right) \\
& + \frac{1}{f} \left( 1 + \frac{1}{r} \frac{\omega}{\omega_s} n \right) \phi^2 , \tag{B11}
\end{aligned}$$

$$\begin{aligned}
0 = & \frac{f}{l g} \left( \partial_r^2 \omega_s + \frac{2}{r} \partial_r \omega_s + \frac{1}{2 l} \partial_r l \partial_r \omega_s \right) \\
& + \frac{1}{r^2} \frac{f}{l g} \left( \partial_\theta^2 \omega_s + \frac{\cos \theta}{\sin \theta} \partial_\theta \omega_s + \frac{1}{2 l} \partial_\theta l \partial_\theta \omega_s \right) . \tag{B12}
\end{aligned}$$

## APPENDIX C: STRESS-ENERGY-TENSOR

### 1. Spherically symmetric solutions

The nonvanishing components of the stress-energy–tensor for non-rotating boson stars read

$$T_{tt} = \left( f U(\phi) + \omega_s^2 \phi^2 + \frac{f^2}{l} (\partial_r \phi)^2 \right) \tag{C1}$$

$$T_{rr} = - \left( \frac{l}{f} U(\phi) - \frac{l}{f^2} \omega_s^2 \phi^2 - (\partial_r \phi)^2 \right) \tag{C2}$$

$$T_{\theta\theta} = -r^2 \left( \frac{l}{f} U(\phi) - \frac{l}{f^2} \omega_s^2 \phi^2 + (\partial_r \phi)^2 \right) \tag{C3}$$

$$T_{\varphi\varphi} = -r^2 \sin^2 \theta l \left( \frac{1}{f} U(\phi) - \frac{1}{f^2} \omega^2 \phi^2 + \frac{1}{l} (\partial_r \phi)^2 \right) \tag{C4}$$

## 2. Axially symmetric solutions

The nonvanishing components of the stress-energy–tensor for rotating boson stars read

$$\begin{aligned}
T_{tt} = & \left[ f U(\phi) - \sin^2 \theta \frac{l}{f} \omega^2 U(\phi) \right. \\
& + \omega_s^2 \phi^2 - \frac{2}{r} \omega n \omega_s \phi^2 + \frac{1}{r^2 \sin^2 \theta} \frac{f^2}{l} n^2 \phi^2 \\
& + \frac{2}{r} \sin^2 \theta \frac{l}{f^2} \omega^3 n \omega_s \phi^2 + \sin^2 \theta \frac{l}{f^2} \omega^2 \omega_s^2 \phi^2 \\
& - \frac{2}{r^2} \omega^2 n^2 \phi^2 + \frac{1}{r^2} \sin^2 \theta \frac{l}{f^2} \omega^4 n^2 \phi^2 \\
& + \frac{f^2}{l g} (\partial_r \phi)^2 - \sin^2 \theta \frac{1}{g} \omega^2 (\partial_r \phi)^2 \\
& \left. + \frac{1}{r^2} \frac{f^2}{l g} (\partial_\theta \phi)^2 - \frac{1}{r^2} \sin^2 \theta \frac{l}{g} \omega^2 (\partial_\theta \phi)^2 \right] \quad (C5)
\end{aligned}$$

$$\begin{aligned}
T_{rr} = & \left[ -\frac{lg}{f} U(\phi) + \frac{lg}{f^2} \omega_s^2 \phi^2 + \frac{2}{r} \frac{lg}{f^2} \omega n \omega_s \phi^2 \right. \\
& - \frac{1}{r^2 \sin^2 \theta} g n^2 \phi^2 + \frac{1}{r^2} \frac{lg}{f^2} \omega^2 n^2 \phi^2 \\
& \left. + (\partial_r \phi)^2 - \frac{1}{r^2} (\partial_\theta \phi)^2 \right] \quad (C6)
\end{aligned}$$

$$T_{r\theta} = \left[ 2 (\partial_r \phi) (\partial_\theta \phi) \right] \quad (C7)$$

$$\begin{aligned}
T_{\theta\theta} = & \left[ -r^2 \frac{lg}{f} U(\phi) + r^2 \frac{lg}{f^2} \omega_s^2 \phi^2 \right. \\
& + 2r \frac{lg}{f^2} \omega n \omega_s \phi^2 + \frac{lg}{f^2} \omega^2 n^2 \phi^2 \\
& \left. - \frac{1}{\sin^2 \theta} g n^2 \phi^2 - r^2 (\partial_r \phi)^2 + (\partial_\theta \phi)^2 \right] \quad (C8)
\end{aligned}$$

$$\begin{aligned}
T_{t\varphi} = & \left[ r \sin^2 \theta \frac{l}{f} \omega U(\phi) - r \sin^2 \theta \frac{l}{f^2} \omega \omega_s^2 \phi^2 \right. \\
& - 2 \sin^2 \theta \frac{l}{f^2} \omega^2 n \omega_s \phi^2 + \frac{1}{r} \omega n^2 \phi^2 \\
& - \frac{1}{r} \sin^2 \theta \frac{l}{f^2} \omega^3 n^2 \phi^2 + 2n \omega_s \phi^2 \\
& \left. + r \sin^2 \theta \frac{1}{g} \omega (\partial_r \phi)^2 + \frac{1}{r} \sin^2 \theta \frac{1}{g} \omega (\partial_\theta \phi)^2 \right] \quad (C9)
\end{aligned}$$

$$\begin{aligned}
T_{\varphi\varphi} = & \left[ -r^2 \sin^2 \theta \frac{l}{f} U(\phi) + r^2 \sin^2 \theta \frac{l}{f^2} \omega_s^2 \phi^2 \right. \\
& + 2r \sin^2 \theta \frac{l}{f^2} \omega n \omega_s \phi^2 + n^2 \phi^2 \\
& + \sin^2 \theta \frac{l}{f^2} \omega^2 n^2 \phi^2 \\
& \left. - r^2 \sin^2 \theta \frac{1}{g} (\partial_r \phi)^2 - \sin^2 \theta \frac{1}{g} (\partial_\theta \phi)^2 \right] . \tag{C10}
\end{aligned}$$

---

[1] R. Friedberg, T. D. Lee and A. Sirlin, Phys. Rev. D13, 2739 (1976)

[2] S. Coleman Nucl. Phys. B262, 263 (1985) (E: B269, 744 (1986))

[3] T. D. Lee, and Y. Pang, Phys. Rept. 221, 251 (1992)

[4] M. S. Volkov and E. Wöhnert, Phys. Rev. D66, 085003 (2002)

[5] F. E. Schunck and E. W. Mielke, in *Relativity and Scientific Computing*, edited by F. W. Hehl, R. A. Puntigam and H. Ruder (Springer, Berlin, 1996), 138

[6] R. Friedberg, T. D. Lee and Y. Pang, Phys. Rev. D35, 12 (1987)

[7] P. Jetzer, Phys. Rept. 220, 163 (1992)

[8] E. Mielke and F. E. Schunck, gr-qc/9801063

[9] F. E. Schunck and E. W. Mielke, Nucl. Phys. B564, 185 (2000)

[10] E. W. Mielke, and F. E. Schunck, 8th Marcel Grossmann Meeting (MG 8), Jerusalem, Israel, 22-27 Jun 1997, Pt.B 1607 (gr-qc/9801063)

[11] S. Yoshida and Y. Eriguchi, Phys. Rev. D56, 2 (1997)

[12] R. M. Wald, General Relativity (University of Chicago Press, Chicago, 1984)

[13] B. Kleihaus and J. Kunz, Phys. Rev. D57, 834 (1998)

[14] D. Kramer, H. Stephani, E. Herlt, and M. MacCallum, Exact Solutions of Einstein's Field Equations, (Cambridge University Press, Cambridge, 1980)

[15] B. Kleihaus and J. Kunz, Phys. Rev. Lett. 86, 3704 (2001)

[16] B. Kleihaus, J. Kunz, and F. Navarro-Lérida, Phys. Rev. D66, 104001 (2002)

[17] U. Ascher, J. Christiansen, R. D. Russell, A collocation solver for mixed order systems of boundary value problems, Mathematics of Computation 33, 659 (1979)

U. Ascher, J. Christiansen, R. D. Russell, Collocation software for boundary-value ODEs, ACM Transactions 7, 209 (1981)

[18] In all formulae of [4] based on the scalar field equation a factor of two is missing in front of the potential  $U$ .

[19] The numerical solutions shown in [4] can be considered as obtained with a potential differing from the true potential by a factor of two. The expression for the mass employed in [4] contains, however, the true potential, leading to an inconsistency of the values quoted in the Tables of [4].

[20] When following the spirals towards their centers, we observe convergence of the mass, the charge and the frequency to finite limiting values. At the same time the functions approach limiting functions. These limiting functions consist of two parts. In the exterior part the limiting solutions correspond to Schwarzschild solutions, in the interior part we have not succeeded in determining the limiting solutions numerically.

[21] Trying to again use a scaling argument to construct the solutions in the interval  $[\omega_0(0), \omega_{\min}]$  in the limit  $\kappa \rightarrow 0$ , one can use  $\hat{r} = \sqrt{\kappa}r$  to obtain a new set of two differential equations for the metric functions together with a constraint for the scalar field, valid in an interval  $[0, \hat{r}_0]$ , where  $\hat{r}_0$  depends on the frequency  $\omega_s$ . Unfortunately, we have not succeeded in determining the dependence  $\hat{r}_0(\omega_s)$ .

[22] W. Schönauer and R. Weiß, J. Comput. Appl. Math. 27, 279 (1989)

M. Schauder, R. Weiß and W. Schönauer, The CADSOL Program Package, Universität Karlsruhe, Interner Bericht Nr. 46/92 (1992).